Highly reproducible tissue positioning with tapered pillar design in engineered heart tissue platforms

Dostanic, Milica; Windt, Laura; Wiendels, Maury; van Meer, Berend J.; Mummery, Christine L.; Sarro, Pasqualina M.; Mastrangeli, Massimo

DOI
10.1109/MEMS49605.2023.10052166

Publication date
2023

Document Version
Final published version

Published in
Proceedings of the 2023 IEEE 36th International Conference on Micro Electro Mechanical Systems (MEMS)

HIGHLY REPRODUCIBLE TISSUE POSITIONING WITH TAPERED PILLAR DESIGN IN ENGINEERED HEART TISSUE PLATFORMS

Milica Dostanić[1,2], Laura M. Windt[2], Maury Wiendels[2], Berend J. van Meer[2], Christine L. Mummery[2,3], Pasqualina M. Sarro[1] and Massimo Mastrangeli[1]

[1] Microelectronics, TU Delft, Delft, The Netherlands

[2] Anatomy and Embryology, LUMC, Leiden, The Netherlands

[3]Applied Stem Cell Technology, University of Twente, Enschede, The Netherlands

2023 IEEE 36th International Conference on Micro Electro Mechanical Systems (MEMS) | 978-1-6654-9308-6/23/$31.00 ©2023 IEEE | DOI: 10.1109/MEMS49605.2023.10052166

ABSTRACT

We present a novel design of elastic micropillars for tissue self-assembly in engineered heart tissue (EHT) platforms. The innovative tapered profile confines reproducibly the tissue position along the main micropillar axis, increasing the accuracy of tissue contraction force measurement. Polydimethylsiloxane-based pillars were designed and fabricated by wafer-level molding in an hourglass shape, with symmetric tapering producing a restriction for tissue movement in the middle of the pillars' length. Confinement efficacy of the new geometry was validated by comparing the tissue performance in straight versus tapered (75° or 80° tapering angle) micropillars. While in all three cases compact tissues formed successfully, for both tapered designs the functionality assays evidenced yield increase from 15% to 100%, higher spatial tissue confinement, and correspondingly higher accuracy and smaller dispersion in measurements of tissue contraction force.

KEYWORDS

engineered heart tissue, heart-on-chip, organ-on-chip, microfabrication

INTRODUCTION

Engineered heart tissue (EHT) models have demonstrated valuable potential to reproduce the (patho)physiology of human cardiac tissue *in vitro* [1]. They are composed of cardiomyocytes (CMs) and non-cardiomyocyte cells within an extracellular matrix (ECM), which self-assemble into tissue-like constructs around two or multiple elastic anchoring points, here called (micro)pillars. For a platform meant to culture EHTs, the design of substrate, the shape and number of elastic pillars, and their mechanical properties are crucial for tissue formation. In our previous miniature EHT platform based on polydimethylsiloxane (PDMS)[2], the cell-gel mixture self-assembled into a tissue-like construct around a pair of micropillars with uniform, rectangular cross-section within an elliptic microwell. However, tests showed that such straight pillar geometry is not optimal for long-term tissue culture, as tissues tend in time to increase the contraction force and move upwards towards the pillars' tip, eventually jumping off and detaching from the pillars in extreme cases. Variation in tissues' adherence position along the pillars hampers precise and consistent measurements of tissue contractile parameters. To address this issue, herein we introduce a tailored tapering in pillar design to constrain the tissue on a precisely defined position along the pillars' length.

DESIGN OF TAPERED PILLARS

The tapered design of pillars aims to pre-determine the tissue position over time. This increased positional control is achieved by providing mechanical resistance against tissue movement outside of the intended region. Moreover, the new design aims to preserve the volume of the elliptic well (2 µL) and pillar stiffness close to that of the previously developed pillars [2]. Additionally, tapering should provide mechanical constraint to the tissue movement in the middle of the pillars' length, without affecting significantly the dynamics of tissue formation observed in the previously developed models.

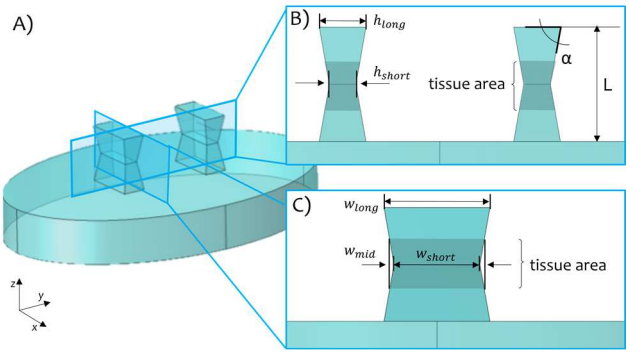

Figure 1. Design and geometrical parameters of tapered pillars implemented in Comsol Multiphysics: A) 3D geometry of tapered pillars on PDMS substrate; B) cross-section of the pillars along the y axis; C) cross-section of pillars along the x axis.

To meet these requirements, an hourglass pillar profile with central symmetric tapering was introduced, whereby the pillar walls form a 75º or 80º angle α with the horizontal planes (Fig. 1). Such a profile is chosen as a compromise between sharper angles that provide stricter mechanical confinement and an angle close to 90º that enables easy removal of PDMS structures from the mould. The dimensions of the pillars for both tapering angles were determined from numerical simulations implemented in Comsol Multiphysics®. Cross-sections and all relevant dimensions of the tapered pillars are shown in Fig. 1 and the values given in Table 1. These dimensions were used to design masks for the platform microfabrication.

Table 1 Design parameters for the tapered pillars.

Symbol	Description	Value	
α [deg]	tapering angle	80	75
h_{short} [μm]	pillars' middle thickness	142	157
h_{long} [μm]	pillars' tip thickness	252	280
w_{short} [μm]	pillars' middle width	383	367
w_{long} [μm]	pillars' tip width	471	447
L [μm]	pillars' length	500	500

FABRICATION

The hourglass profile of tapered pillars was achieved by molding PDMS into a Si substrate processed on both sides by alternating anisotropic deep reactive ion etching (DRIE, Bosch process) and isotropic etching of silicon. Such etching approach creates a staircase-like profile while precisely defining the tapering angle of the etched holes and the location of their conjunction [3], [4]. Fine tuning of the tapering angle was controlled by knowing the etch rates of both isotropic and anisotropic etching processes. The tapering angle α (Fig. 1.B) can be calculated according to the following relation:

$$tg\alpha = \frac{c_B \cdot r_B(z) + t_{iso} \cdot r_{iso}^{\downarrow}(z)}{(t_{iso} - t_{C_4F_8}) \cdot r_{iso}^{\rightarrow}(z)}$$

Here c_B is the total number of Bosch cycles, t_{iso} is the duration of isotropic etch, and $t_{C_4F_8}$ is the time required to remove the residual C_4F_8 layer from the sidewalls after the Bosch process. Vertical etch rate of the Bosch process, as well as vertical and lateral isotropic etch rates, are defined as r_B, $r_{iso}^{\downarrow}$ and $r_{iso}^{\rightarrow}$, respectively. All etching parameters are highly dependent on process temperature, geometry of the masks (density of structures) and depth of etching, which requires etch rate adjustments per each etching cycle.

Fabrication of the mould for tapered pillars started from plasma-enhanced chemical vapor deposition (PECVD) of a 5 µm-thick oxide layer on a double-side polished, 500 µm-thick Si wafer. The oxide layer was patterned using standard photolithography and dry etching to create a two-step hard mask for DRIE, on both wafer sides (Fig. 2.1). In the patterning, the windows in the first mask determined the narrow rectangular shapes which defined the middle part of the pillars. The larger windows of the second mask defined the top and bottom dimensions of the micropillars at the final etching stage, and fine-tuned the tapering angle.

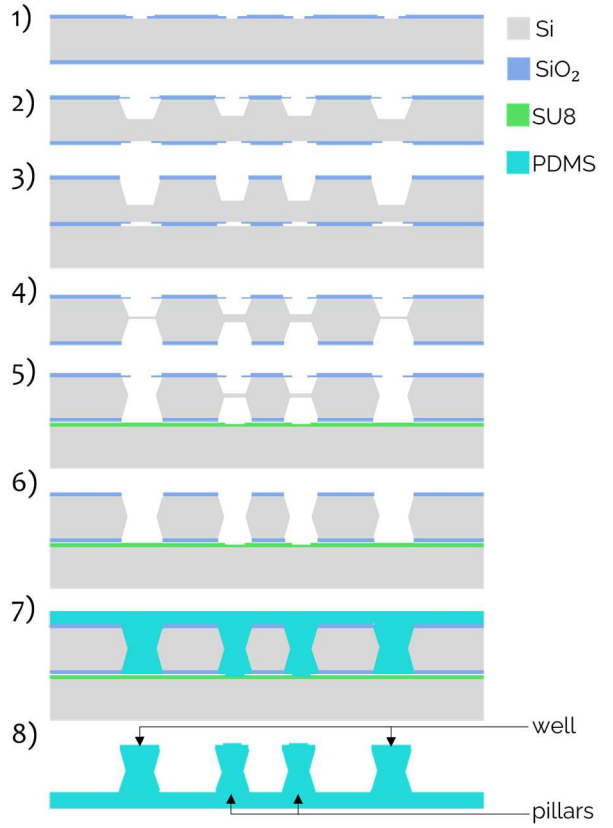

Figure 2. Sketch of the fabrication process of the PDMS-based EHT platform with tapered pillars: 1) definition of SiO_2 hard mask; 2-4) DRIE of tapered holes into the Si mold; 5) wafer bonding; 6) etching finalization of the tapered structures; 7) PDMS molding; 8) released EHT platforms with tapered pillars

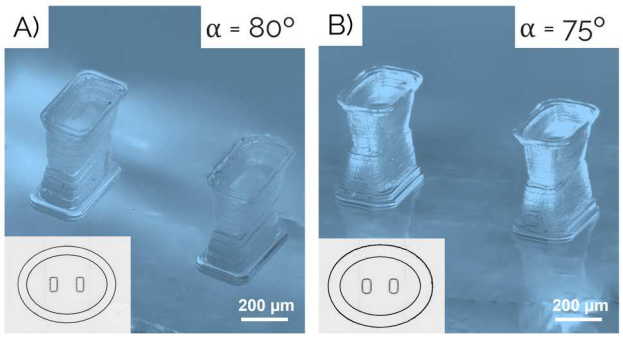

Figure 3. Optical images of PDMS tapered pillars released from the silicon mould, with two different tapering angles: A) α=75° and B) α=80°. Top view of the platforms with elliptic microwell are shown in the insets.

After hard mask definition, DRIE etching followed, yielding a scalloped, staircase-like profile. First, the front side of the wafer was etched by alternating Bosch process and isotropic etching, until reaching a depth of 240 µm (Fig. 2.2). For the last 20 µm of the front-side etch, the inner part of the hard mask was removed by wet etching of SiO_2 in a buffered HF solution. Frontside DRIE was finalized by transferring the process wafer on a Si carrier wafer (Fig. 2.3). Transfer to the carrier wafer ensured the same etching conditions on both front- and backside of the process wafer, and thus symmetry of tapered shapes. After etching, the wafer was cleaned in O_2 plasma to remove polymer residues from the Bosch process.

The same etching strategy was applied to the backside, until reaching a depth of 200 µm (Fig. 2.4). However, finalization of etching required bonding the process wafer to a support wafer to enclose etched pillars and wells from one side. Direct wafer bonding was performed using an adhesive polymer as intermediate layer in between the two silicon wafers (Fig. 2.5). In this case, SU8 – an epoxy-based negative resist – was used as the bonding adhesive, spin-coated and soft-baked on the support Si wafer. The bonding was performed by applying 2.5 kN force on the wafers, which enabled wetting of the Si surface of the process wafer by the SU8 layer. In this configuration, final cross-linking and hard baking of SU8 were performed at 120 °C, to ensure strong and reliable wafer bonding. Once bonding was completed, etching could be finalized to merge the tapered holes in the middle of the wafer (Fig 2.6).

The final step of the fabrication is PDMS moulding. Prior to polymer spin-coating, the wafer surface was made hydrophobic by adsorbing a self-assembled monolayer of perfluorosilane from vapor phase. Elastomer mixed with the curing agent in 10:1 ratio was spin-coated for 30 s at 400 rpm on top of the Si mould (Fig. 2.7). After degassing and curing at 90 °C for 1 h, PDMS structures were released from the mould (Fig. 2.8). Both tapered pillar structures were optically characterized using optical profilometry and the corresponding images are shown in Fig. 3.

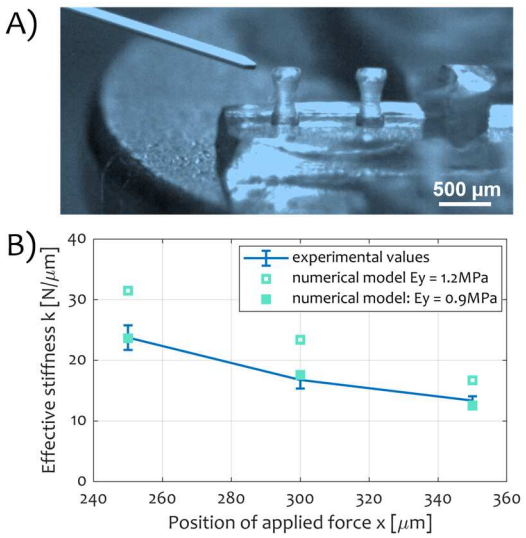

Figure 4. A) Setup for the mechanical characterization of the elastic micropillars using nanoindentation; B) Stiffness analysis for 80° tapered pillars. Data from finite element simulations (green) compared and fitted to the measured data (blue) to estimate the actual Young's modulus of PDMS.

MECHANICAL CHARACTERIZATION

A FemtoTools Nanomechanical Testing System (FT-NMT03) was used for the mechanical characterization of the tapered pillars [2]. A silicon cantilever with flat circular tip, 50 µm in diameter, was used to apply force on different positions along the pillars length. The setup is illustrated in Fig. 4A. Measurements were performed on 3 different positions on each pillar, and repeated for 3 samples of both 75° and 80° tapered pillars. The maximum applied force was 80 µN and the pillars were displaced accordingly. The corresponding displacement–force curve was obtained by measuring the pillars' displacement with a piezo scanner. The stiffness of pillars in the point of force application was obtained from the unloading curve upon pillars' return to the initial position. The measured pillar stiffness was 14 N/m and 16 N/m for 80° and 75° tapered designs, respectively, compared to 10 N/m for 90° straight pillars.

Nanoindentation measurements were used to calculate the Young's modulus (E_Y) of the PDMS and to compare their elastic response curve to the ones obtained from numerical and analytical models. Both models assumed E_Y = 1.2 MPa. The conditions from the experimental setup were recreated in Comsol to enable data comparison. The shift between measured values and simulations for E_Y = 1.2 MPa is noticeable from Fig. 4B. This shift was corrected by finding the value of E_Y that minimizes the mean square difference between the values in both curves. The new value of E_Y was found to be 900 KPa, for both 80° and 75° pillars. Comparison of measured and simulated values, before and after Young's modulus correction for the case of 80° tapered pillars is shown in Fig 4B.

INCLUSION OF CARDIAC CELLS

The assessment of the novel pillar design efficiency was performed by culturing EHTs on both tapered designs and comparing them to the tissue performance in the case of straight pillars. The main questions of the study were the efficiency of tissue confinement in tapered design and its effect on the tissue contractile properties, yield of the experiment, and variation of the results.

For EHT formation on tapered pillars the same protocol was used as reported previously [5]. Briefly, three different cell types: cardiac fibroblast (cFB), endothelial cells (ECs) and cardiomyocytes (CMs) were derived from an hiPSC line (LUMC0020iCTRL-06). The hiPSCs were differentiated into CMs as described previously [6]. The EHTs were composed from 70% hiPSC-CMs,15% hiPSC-derived cFB and 15% ECs. For the ECM gel mixture, 41% of acid solubilized collagen I (3.3 mg/mL), 5% of DMEM (10X), 6% of NaOH, 9% of growth factor reduced Matrigel and 39% of formation medium were used. The EHTs were cultured in formation medium for 72 h combined with VEGF (50 ng/mL) and FGF (5 ng/mL). After 72 h the culture medium was switched to MBEL+ VEGF (50 ng/mL)+ FGF (5 ng/mL) and maintained in culture for 14 days. The tissues successfully formed in all three different pillar designs. Representative images of tissues formed around straight, 80° tapered and 75 ° tapered pillars are shown in Fig. 5. Brightfield images were taken live on day 7 since the beginning of the experiment with a Nikon Eclipse Ti2.

To assess tissue confinement with the tapered geometry, the position of the tissue along pillars length were measured for both designs. Optical images were taken using Keyence VHX-900F microscope at 60° angle. The imaging was performed in the end of the experiment, after fixing the tissues on the pillars. The measurements were repeated for at least three tissues of each tapered pillar design, and confinement in the middle of pillars was observed in all of them. In Fig. 6 representative examples of tissue confinement in the middle region are shown. By visual inspection it was determined that the new geometry successfully provided mechanical constraints for the tissue movement outside of the narrow area in the middle of the pillars.

The comparative study between tapered and straight pillar designs was performed based on the yield of the experiment and contractile tissue parameters. The yield of the experiment increased from 15% for the straight design to 100% for both 80° and 75° tapered pillars. All tissues from tapered designs reached the end point of the experiment, proving that spatial confinement solved the problem of tissue jumping off and enabled long-term cell culture. The duration of the experiment was 14 days.

The contractile parameters of tissues in different pillars were measured. Videos of contracting tissues were recorded on day 4, 7 and 11, during spontaneous contraction

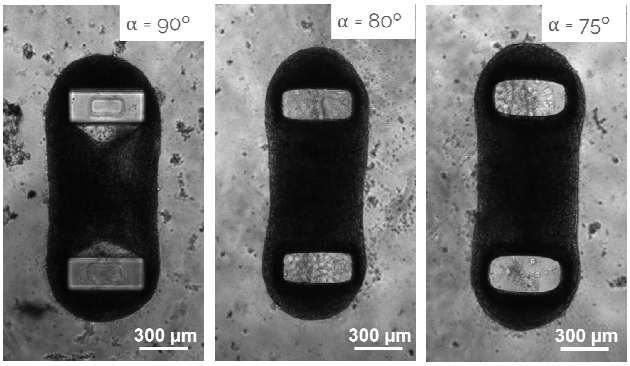

Figure 5. Brightfield imaging of EHT formation around straight pillars (i.e., α=90°) and both versions of tapered pillars (α=80° and α=75°). Tissue shown in black.

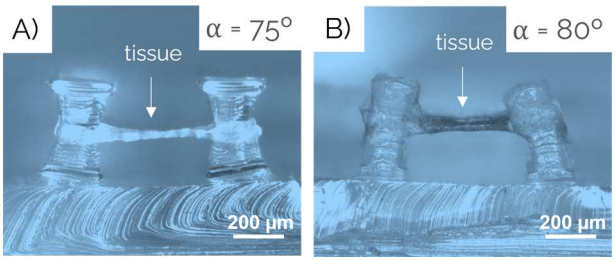

Figure 6. Example of spatial confinement of tissues in the middle of pillar length in both A) 75° and B) 80° tapered designs.

as well as during electrical pacing at 1 Hz and 2 Hz. Videos of contracting tissues of 10 s duration were recorded using an inverted optical microscope (Nikon Eclipse Ti2) with a high-speed camera. The videos were analyzed using a custom-made standalone app for tissue contractile performance assessment, by tracking the displacement of pillars tips. The results of the analysis and comparison of all three designs on day 7 are shown in Fig. 7.

From the graphs it can be noticed that the variability in the contractile behavior is reduced (by 85%) in case of both tapered pillar designs compared to the straight ones. The other parameters describing contractile kinetics, such as contraction and relaxation time to reach 10% and 90% of the upstroke and downstroke of the contraction cycle, are comparable in all three designs. It is yet to be determined to which extent the decrease in variability of contractile properties can be attributed to the new pillar design and tissue confinement or to the increase in stiffness of the tapered pillars compared to previous designs.

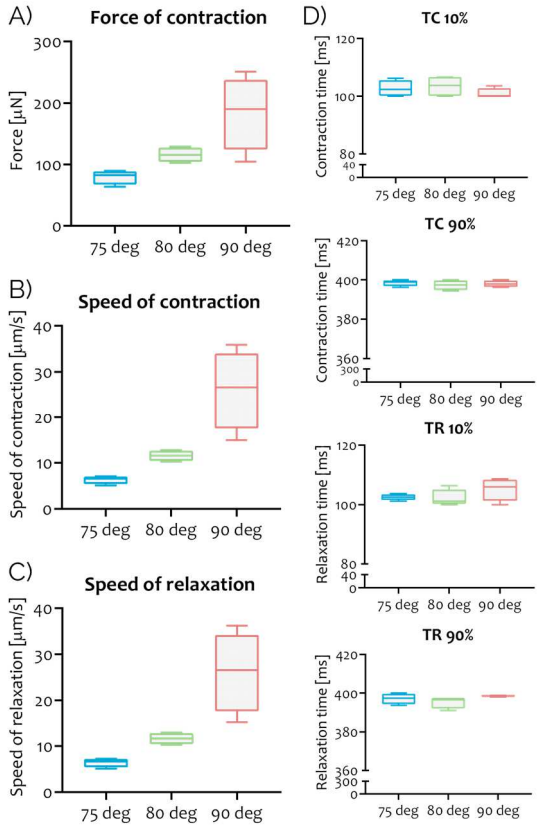

Figure 7. Comparison of contractile performance of tissues on straight and tapered pillars: (A) Contractile force of EHTs; contraction (B) and relaxation velocity (C) of EHTs over time. (D) Time of contraction (TC) and relaxation (TR) to reach 10% and 90% of the upstroke and downstroke of the contraction cycle.

CONCLUSIONS

We presented a novel design of PDMS pillars for tissue self-assembly in EHT platforms. The design is meant to increase the control over tissue position over time and consequently reproducibility of contraction force measurements. PDMS-based pillars were designed and fabricated in an hourglass shape, with symmetric tapering, producing a restriction in the middle of the pillars' length. The pillars were fabricated with two different tapering angles to test their confinement efficiency. In addition, mechanical characterization of both tapered designs was performed using a nanoindentation measurement system. This resulted in correction of the assumed Young's modulus and consequently precise measurements of force of contraction.

The efficiency of new designs in tissue confinement was tested by performing a comparative study between straight and both tapered pillar designs. It was noticed that the tissue formation was unaffected by the new pillar design. Tissue confinement was confirmed optically for both tapered designs. Consequently, the yield of experiments significantly increased, and the issue of tissues jumping off the pillars was solved for this specific EHT platform. Furthermore, the effect of the tapered design on tissue contractile properties was analyzed. A decrease in variability of the contractile force measurements was observed, while the other contractile kinetic parameters were comparable in all three designs.

ACKNOWLEDGEMENTS

The authors thank the staff at the Else Kooi Laboratory of TU Delft for their support with microfabrication. This work was supported by the Netherlands Organ-on-Chip Initiative, an NWO gravitation project funded by the Ministry of Education, Culture and Science of the government of the Netherlands (024.003.001).

REFERENCES

[1] J. M. Stein, C. L. Mummery, and M. Bellin, "Engineered models of the human heart: Directions and challenges," *Stem Cell Rep.*, vol. 16, no. 9, pp. 2049–2057, Sep. 2021.

[2] M. Dostanić *et al.*, "A Miniaturized EHT Platform for Accurate Measurements of Tissue Contractile Properties," *J. Microelectromechanical Syst.*, vol. 29, no. 5, pp. 881–887, Oct. 2020.

[3] R. Li, Y. Lamy, W. F. A. Besling, F. Roozeboom, and P. M. Sarro, "Continuous deep reactive ion etching of tapered via holes for three-dimensional integration," *J. Micromech. Microeng.*, vol. 18, no. 12, p. 125023, Nov. 2008,

[4] Z. Ren and M. E. McNie, "Inductively coupled plasma etching of tapered via in silicon for MEMS integration," *Microelectron. Eng.*, vol. 141, pp. 261–266, Jun. 2015.

[5] A. Hansen *et al.*, "Development of a drug screening platform based on engineered heart tissue," *Circ. Res.*, vol. 107, no. 1, pp. 35–44, Jul. 2010.

[6] E. Giacomelli *et al.*, "Human-iPSC-Derived Cardiac Stromal Cells Enhance Maturation in 3D Cardiac Microtissues and Reveal Non-cardiomyocyte Contributions to Heart Disease," *Cell Stem Cell*, vol. 26, no. 6, pp. 862-879.e11, Jun. 2020.